

Key Role of the North Pacific Oscillation–West Pacific Pattern in Generating the Extreme 2013/14 North American Winter

STEPHEN BAXTER

Climate Prediction Center, NOAA/NWS/NCEP, College Park, Maryland

SUMANT NIGAM

University of Maryland, College Park, College Park, Maryland

(Manuscript received 19 October 2014, in final form 12 June 2015)

ABSTRACT

The 2013/14 boreal winter (December 2013–February 2014) brought extended periods of anomalously cold weather to central and eastern North America. The authors show that a leading pattern of extratropical variability, whose sea level pressure footprint is the North Pacific Oscillation (NPO) and circulation footprint the West Pacific (WP) teleconnection—together, the NPO–WP—exhibited extreme and persistent amplitude in this winter. Reconstruction of the 850-hPa temperature, 200-hPa geopotential height, and precipitation reveals that the NPO–WP was the leading contributor to the winter climate anomaly over large swaths of North America. This analysis, furthermore, indicates that NPO–WP variability explains the most variance of monthly winter temperature over central-eastern North America since, at least, 1979. Analysis of the NPO–WP related thermal advection provides physical insight on the generation of the cold temperature anomalies over North America. Although NPO–WP's origin and development remain to be elucidated, its concurrent links to tropical SSTs are tenuous. These findings suggest that notable winter climate anomalies in the Pacific–North American sector need not originate, directly, from the tropics. More broadly, the attribution of the severe 2013/14 winter to the flexing of an extratropical variability pattern is cautionary given the propensity to implicate the tropics, following several decades of focus on El Niño–Southern Oscillation and its regional and far-field impacts.

1. Introduction

The 2013/14 winter (December 2013–February 2014) was anomalously cold across large swaths of central-eastern North America. Multiple, intense cold snaps prompted prolonged media attention, sent energy prices skyward, and led to scientific hypotheses on the cause of an extreme regional winter season in an otherwise warming global climate (e.g., Palmer 2014). A careful analysis of the established winter patterns of monthly atmospheric circulation variability and their near-surface temperature footprints attributes the 2013/14 extreme winter across North America, largely, to the North Pacific Oscillation–West Pacific pattern.

The NPO–WP acronym is used for North Pacific Oscillation (NPO) and the West Pacific (WP) teleconnection pattern. The North Pacific Oscillation, a north–south seesaw in winter sea level pressure over the North Pacific on monthly (and shorter) time scales, was identified by Sir Gilbert Walker in 1924 (Walker 1924). The NPO was known to synoptic forecasters of the U.S. Weather Bureau as early as 1916 because of its significant influence on U.S. winter weather. They noted that the oscillation phase with higher pressure over Alaska and lower pressure over Hawaii was linked with colder conditions over eastern North America, much as during the 2013/14 winter. The WP pattern was defined by Wallace and Gutzler (1981) from teleconnection analysis of the midtropospheric geopotential height field in boreal winter. It consists of a north–south dipole over the western-central Pacific basin in the Northern Hemisphere. Later analysis showed the WP and NPO to be essentially the same variability, with the NPO being the sea level pressure reflection of the WP

Corresponding author address: Sumant Nigam, Department of Atmospheric and Oceanic Science, University of Maryland, College Park, 3419 Computer and Space Science Building, College Park, MD 20742-2425.
E-mail: nigam@umd.edu

geopotential height pattern (Wallace and Gutzler 1981; Nigam 2003; Linkin and Nigam 2008; Nigam and Baxter 2015).

The NPO–WP variability pattern is the Pacific basin analog of the North Atlantic Oscillation (NAO; Nigam 2003). Both consist of a north–south dipole in sea level pressure and tropospheric height anomalies across their basins as well as latitudinal displacement of the climatological jet streams. Not surprisingly, each alters the storm tracks near and downstream of their centers of action, with the NAO impacts pronounced over far eastern North America and Europe, and the NPO–WP ones influential over northeastern Asia and North America. Large amplitude monthly and seasonal geopotential height anomalies resembling the WP pattern would thus be well positioned to significantly impact the surface climate over North America—the case in the 2013/14 winter.

Some recent studies have related NPO variability to changes in central Pacific SSTs, namely, central Pacific El Niño events (DiLorenzo et al. 2013; Furtado et al. 2012) but mostly on decadal time scales. Our analysis suggests that links on monthly and seasonal time scales are tenuous at best, as the SST and outgoing longwave radiation (OLR; used as a proxy for tropical convection) footprints of the NPO–WP are weak (correlations of ~ 0.2 or less, not shown).

Another variability pattern of some significance in the 2013/14 winter is the tropical Northern Hemisphere (TNH) pattern. The TNH was identified by Mo and Livezey (1986), and related to El Niño–Southern Oscillation (ENSO) variability. However, Nigam (2003) showed ENSO’s extratropical winter response to be distinct from the TNH pattern. Rotated empirical orthogonal function (EOF) analysis of 200-hPa heights [as in this study, and in Nigam (2003)] yields two patterns related to SST variability in the tropical Pacific: 1) a height response in the Western Hemisphere extratropics and global tropics with little subseasonal variability (ENSO’s classic winter season response), and 2) a more extratropically confined response exhibiting greater month-to-month variability (TNH-like pattern).

The objective of this analysis is quantitative attribution of the 2013/14 winter circulation and temperature anomalies over North America. The identification of the key building blocks and related reconstruction provide mechanistic insight on the development of phenomenally cold winter temperatures. Our implication of NPO–WP variability—currently viewed as a mode of internal variability—for the highly abnormal 2013/14 winter has potentially wide-reaching implications for subseasonal-to-seasonal climate predictability. The datasets and analysis methods are briefly discussed next while the obtained findings follow in later sections.

2. Data and methods

The analysis draws on the Climate Forecast System Reanalysis (CFSR; Saha et al. 2010) for 200-hPa geopotential height (Z_{200}), 850-hPa temperature (T_{850}) and winds, and 700-hPa vertical velocity (w_{700}), all at monthly resolution and on a 2.5° global grid. The pentad (i.e., 5-day averaged) T_{850} and 200-hPa streamfunction from the CFSR are used to assess subseasonal variability. The precipitation data (on a 0.5° continental grid) is obtained from NOAA/Climate Prediction Center’s unified gauge-based dataset (Chen et al. 2002). The January 1979–February 2014 period is analyzed, with anomalies defined with respect to the 1981–2010 climatology, as in NOAA’s Climate Diagnostic Bulletin (CDB; the monthly archive is online at http://www.cpc.ncep.noaa.gov/products/CDB/CDB_Archive_pdf/pdf_CDB_archive.shtml).

The NPO–WP is obtained alongside other variability patterns in a rotated EOF analysis of monthly, winter [December–February (DJF)] Z_{200} anomalies in the Northern Hemisphere. The leading eight patterns are rotated using the varimax technique, as in Nigam (2003). In this analysis, the NPO–WP emerges as the third-leading pattern, explaining $\sim 11\%$ of the monthly winter variance, after the NAO ($\sim 17\%$) and ENSO response ($\sim 13\%$) patterns. The TNH is the fifth-leading mode in this analysis, explaining $\sim 6\%$ of the variance.

To assess the contribution of the NPO–WP, TNH, and other variability patterns to the extreme 2013/14 winter, the T_{850} , Z_{200} , and precipitation (and w_{700}) anomalies are reconstructed. Multiplication of each rotated EOF pattern (spatial) with its principal component (time varying) value for the target month, and summing the various EOF contributions yields the reconstructed signal; the principal components (PCs) are orthogonal, facilitating reconstruction. The December 2013, and January and February 2014 reconstructions were averaged to produce the 2013/14 winter season anomalies, discussed in the next section.

To assess subseasonal variability, a similar analysis is performed on the pentad 200-hPa streamfunction (ψ_{200}) anomalies; streamfunction is a preferred variable for analysis of tropical–extratropical interaction. Following Baxter and Nigam (2013), a rotated extended-EOF analysis is conducted to extract the subseasonal modes of spatiotemporal variability. Analysis of ψ_{200} yields a clearer identification of the Madden–Julian oscillation’s (MJO) extratropical response, precluding its aliasing onto the extratropical variability patterns. The 120-day running mean anomaly is removed from data prior to analysis, to filter out interannual variability. The data are “extended” using a five-pentad sampling window. In this analysis, NPO–WP emerges as the fourth-leading

mode, behind two modes that capture the time-lagged MJO response, and the Pacific–North American (PNA) pattern.

While the reconstructions themselves are informative, mechanistic links between the NPO–WP circulation and temperature anomalies over North America are also investigated. To this end, the various terms constituting thermal advection are evaluated for the 2013/14 winter season:

$$-\mathbf{V}_{850}^{\text{NPO-WP}} \cdot \nabla T_{850}^C \quad (\text{A}),$$

$$-\mathbf{V}_{850}^{\text{NPO-WP}} \cdot \nabla T_{850}^{\text{NPO-WP}*} \quad (\text{B}), \quad \text{and}$$

$$-\mathbf{V}_{850}^C \cdot \nabla T_{850}^{\text{NPO-WP}*} \quad (\text{C}).$$

Term A constitutes the advection of climatological T_{850} by the NPO–WP contribution to the 850-hPa wind. Term B represents a quasi-nonlinear advection—of the first-order NPO–WP temperature signal ($T^{\text{NPO-WP}*}$) by the NPO–WP related winds. As the observed NPO–WP T_{850} anomaly is the reconstruction target, it cannot be used here. The first-order temperature signal is estimated, indirectly, from term A using the thermal damping from synoptic transient eddies (Lau 1979).¹ Finally, term C constitutes the advection of the first-order NPO–WP temperature signal by the climatological 850-hPa wind.

3. Results

The 2013/14 winter was characterized by significantly below-normal temperatures across much of North America. The NPO–WP principal component was strongly negative, consistent with higher pressure/heights over Alaska and colder-than-normal temperatures over central-eastern North America. The NPO–WP PC averaged over the three winter months exhibited the most negative seasonal value over the entire analysis period (cf. Fig. 4b). Figure 1a shows the observed T_{850} anomalies, with temperatures as cold as -7°C centered southwest of Hudson Bay. The cold temperatures extend from northwestern Canada southeastward to well-populated parts of the central-eastern United States. Above-normal T_{850} was observed over much of Alaska, the U.S. West Coast, and the southwestern United States. The structure and magnitude of the observed anomalies are closely reconstructed (Fig. 1b) using PCs

of the NPO–WP, NAO, TNH, and east Atlantic (EA; Wallace and Gutzler 1981) patterns; Figs. 1c–f show the individual contributions. The NPO–WP contribution clearly resembles the observed anomaly most closely, followed distantly by the TNH. The red outlined box in the panels marks a region of the northern plains (40° – 55°N , 100° – 80°W) whose area-averaged T_{850} anomalies are used in time series analyses. The region was selected because of its proximity to the core of the cold anomaly and the populated areas in the north central-eastern quadrant of the continent.

Figure 2 displays the 200-hPa geopotential height anomaly for this winter. As in Fig. 1, the reconstructed Z_{200} anomaly is displayed alongside the observed (CFSR) one, along with the individual contributions. As with T_{850} , the NPO–WP’s Z_{200} contribution is dominant over North America and closely similar to the observed anomaly there. Figure 2e indicates that TNH was also a contributor over North America but with significantly smaller amplitudes than NPO–WP. It is worth noting that both NAO and EA patterns were also active, with strong projections on the observed T_{850} and Z_{200} anomalies but in the downstream Atlantic and European sectors.

While bitterly cold temperatures in the central-eastern United States defined the 2013/14 winter, the precipitation anomaly was also notable. Most significant, perhaps, was the anomalously dry winter over the U.S. West Coast, especially California (Fig. 3a). The TNH and NPO–WP contributions can explain most of the observed precipitation deficits extending from the Alaska Panhandle to southern California (Figs. 3a,c,e). In fact, from central California to most of the Alaska Panhandle, those two patterns account for over 75% of the observed precipitation deficit (in some cases the reconstruction yields a deficit higher than observed). Over southern California and the desert southwest, the reconstruction from the TNH and NPO–WP generally explains 50%–75% of the observed precipitation anomalies. Of the two patterns, the TNH explains more variability over California, a region of intense study given the multiyear drought that has gripped this region.

The precipitation signals are consistent with the observed and reconstructed 700-hPa vertical velocity anomalies across western North America (Figs. 3b,d,f). The NPO–WP explains some of the wet signal also along the eastern seaboard, though other variability is clearly more important in that region.

To place the 2013/14 winter in historical context, the time series of the area-averaged T_{850} anomalies over the northern plains (red box, Fig. 1) is examined in Fig. 4b, which also shows the standardized NPO–WP principal component; the two are correlated at 0.69, a high value. The winter exhibiting the most negative seasonal T_{850}

¹The first-order NPO–WP temperature signal $T_{850}^{\text{NPO-WP}*}$ is estimated as $-\mathbf{V}_{850}^{\text{NPO-WP}} \cdot \nabla T_{850}^C \approx -\gamma T_{850}^{\text{NPO-WP}*}$ where the right-hand side represents thermal (Newtonian) damping of lower-tropospheric temperature by synoptic transients. The γ is taken as $(3 \text{ days})^{-1}$ following Lau (1979, see their Table I).

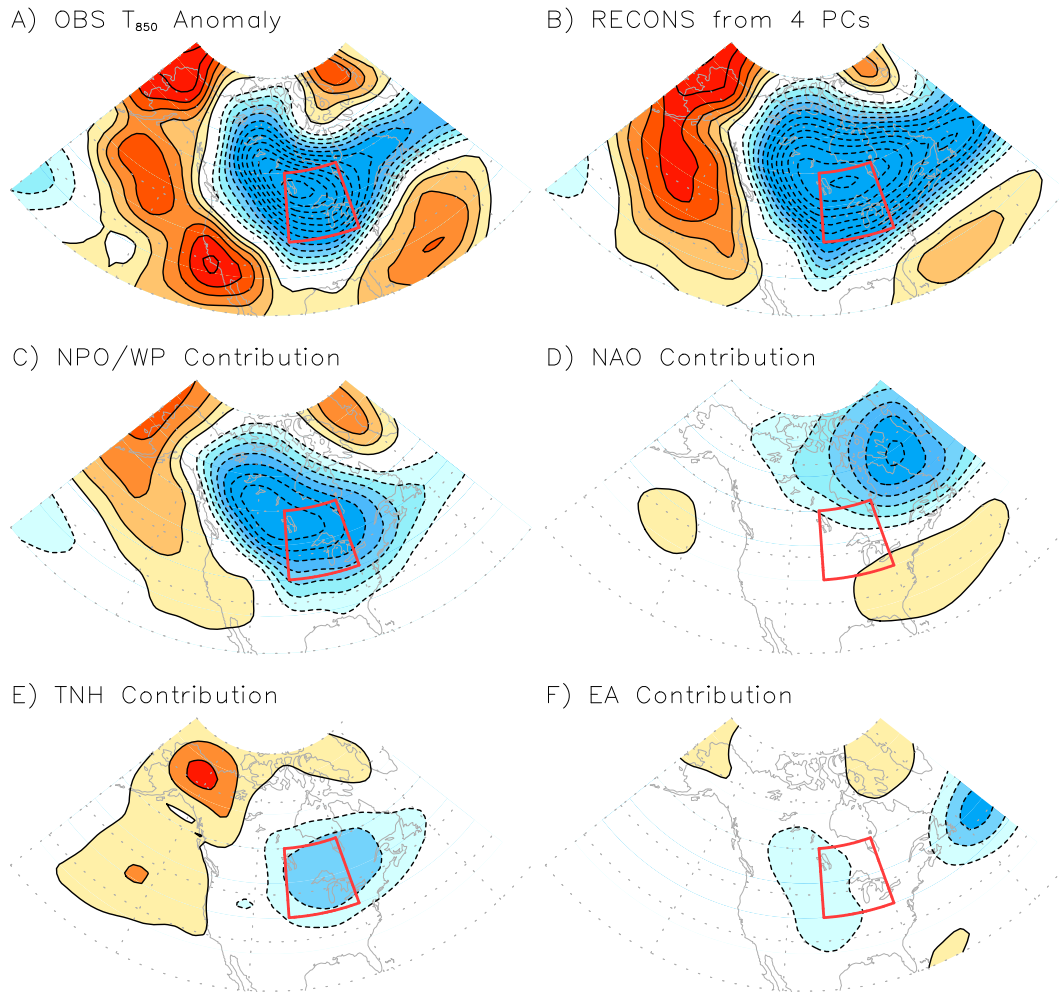


FIG. 1. The 850-hPa temperature anomalies for DJF 2013/14 winter: (a) the observed T_{850} anomaly and the T_{850} anomalies from a reconstruction based on PCs of the Z_{200} variability (see text for analysis details) (b) from four pertinent modes, (c) from NPO–WP, (d) from NAO, (e) from TNH, and (f) from the EA pattern. The T_{850} anomalies are reconstructed by multiplying the Z_{200} PC of each month by its regression pattern. The reconstructed winter month anomalies were then averaged to obtain the winter season (DJF) reconstruction. The contour interval and shading threshold is 0.5 K (zero contour is omitted). The red box (40° – 55° N, 100° – 80° W) marks the northern Great Plains averaging region for the T_{850} anomaly index discussed in subsequent analysis.

anomaly (i.e., most persistently cold) is the 2013/14 one, when the NPO–WP PCs are also most negative. The TNH pattern also contributed to the recent record cold winter (cf. Fig. 1e) but its contribution is secondary to NPO–WP’s pattern. The relative contribution of the two patterns in other extreme winters (when regional T_{850} exceeded plus or minus one standard deviation) is examined via a scatterplot of the two PCs in Fig. 4c. It is noteworthy that every winter month satisfying the threshold for cold (warm) extremeness had a negative (positive) PC value but only in the case of the NPO–WP. The TNH PC was not found as tightly correlated as it exhibits positive values in both cold and warm winters, albeit more often in the cold ones.

The subseasonal variability in the extreme 2013/14 winter over the northern plains is briefly examined in Fig. 4a. The pentad T_{850} anomaly index (standardized) covaries with the pentad NPO–WP principal component, with the exception of the last few pentads. Over this extreme winter, the two pentad indices are correlated at 0.56;² the correlation is 0.45 over all analyzed

² A higher pentad correlation is obtained with T_{850} leading by one pentad. This results from the retrogression of the NPO–WP whose North American center attains peak amplitude in advance of other regions. The NPO–WP PC is, of course, keyed to the overall mature-phase structure. The T_{850} lead over the northern plains is, by no means, indicative of causality; see Fig. 5.

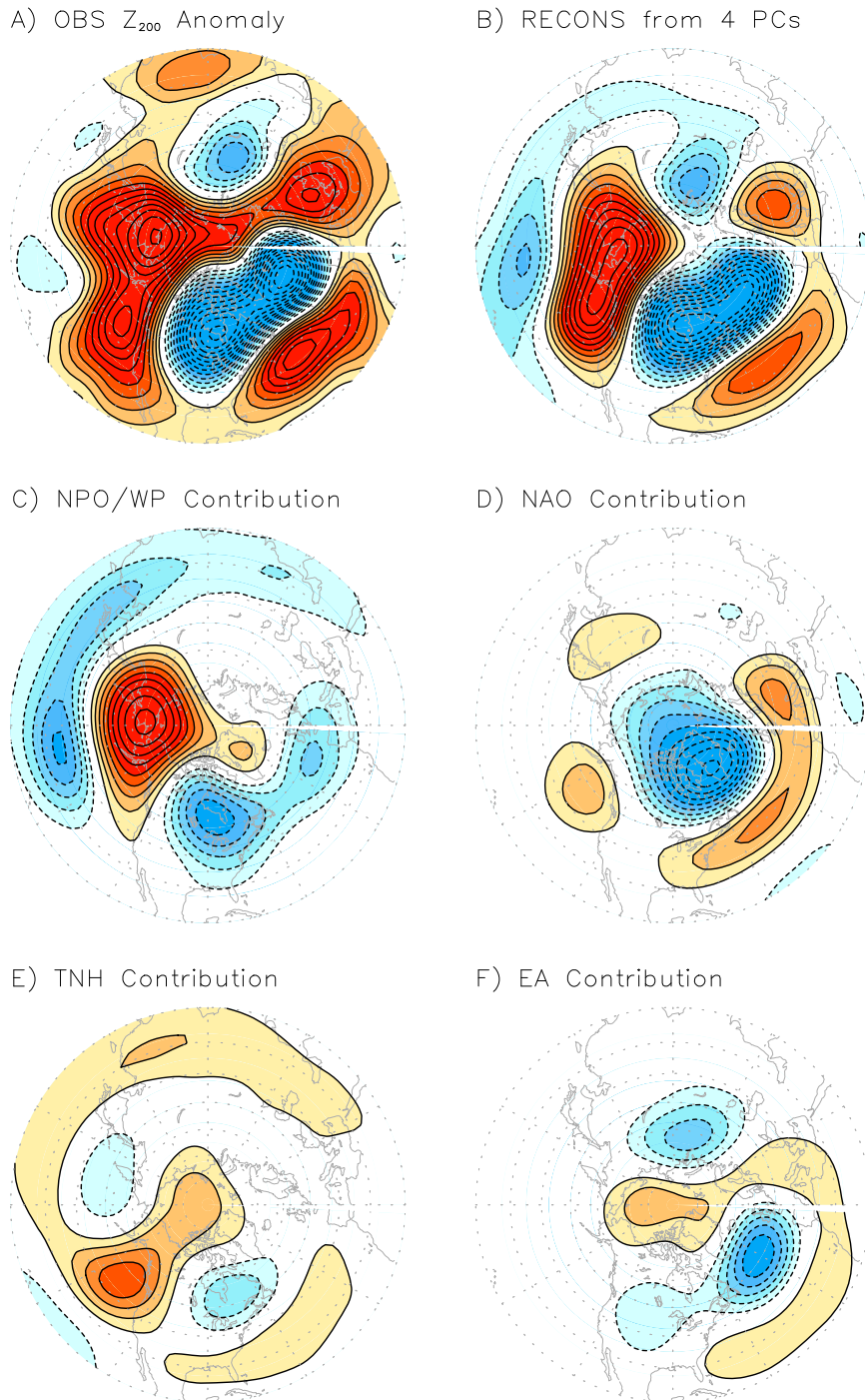


FIG. 2. As in Fig. 1, but for the 200-hPa geopotential height anomalies; contour interval and shading threshold is 15 m. Principal components obtained from the variability analysis of this field are the basis for all reported reconstruction.

winters (1979–2014). The pentad correlation for the 2013/14 winter and across all winters is impressive, highlighting the preeminence of the NPO–WP in influencing the winter surface climate over the northern plains, even on

subseasonal time scales. Correlations in the 0.4–0.6 range also indicate that the NPO–WP influence is far from complete: subseasonally, this is reflected in the near-zero principal component values of NPO–WP during mid-January

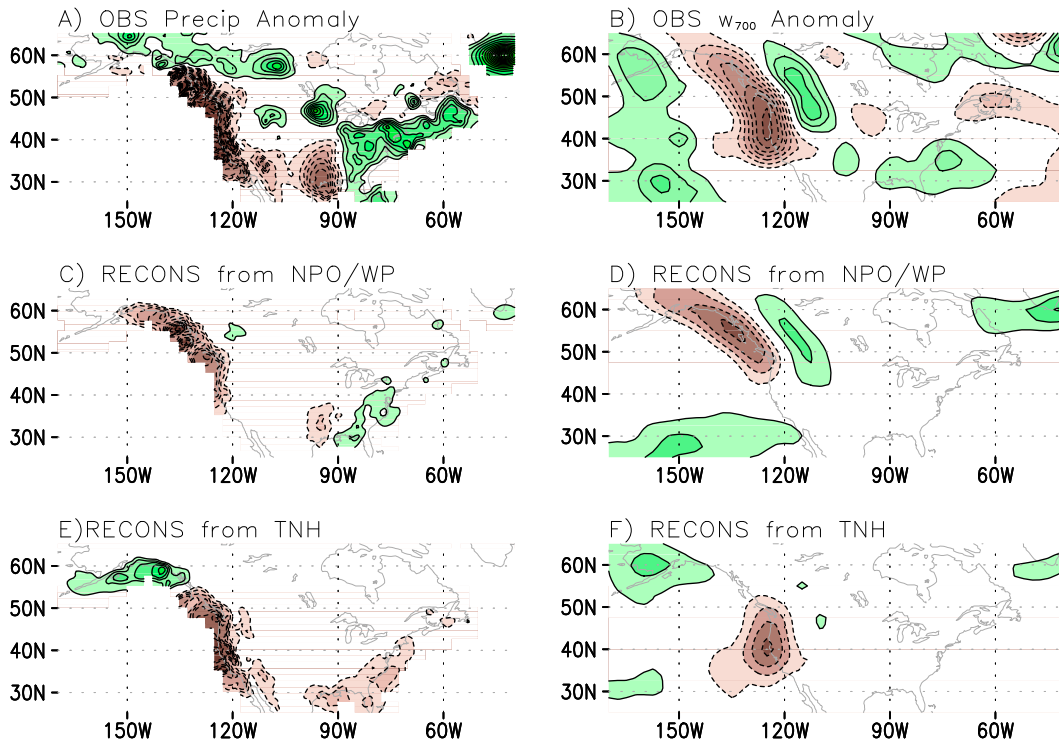


FIG. 3. Precipitation and w_{700} anomalies during DJF 2013/14: (a) observed precipitation anomaly, and its reconstruction from (c) NPO–WP and (e) TNH principal components. (b) Observed w_{700} anomaly, and its reconstruction (d),(f) from the same principal components as in (c),(e), respectively. The contour interval and shading threshold is 0.25 mm day^{-1} for precipitation and 1 cm s^{-1} for w_{700} (zero contour omitted).

of 2014 (cf. Fig. 4a). The significant contribution of TNH variability on monthly time scales was noted earlier.

The observationally rooted analysis presented above attributes the extreme 2013/14 winter temperatures over North America to NPO–WP variability. The statistical attribution is provided a mechanistic underpinning in this section from the elaboration of the temperature advection processes, in particular the phenomenal cold advection experienced by the northern plains and the central-eastern United States. The advection of climatological T_{850} can account for the spatial structure of NPO–WP-related anomalies east of the Rocky Mountains, but not its magnitude (Fig. 5b). Using this field (Fig. 5b) and a 3-day Newtonian damping (to represent thermal damping by synoptic transient eddies), NPO–WP’s first-order T_{850} signal ($T^{\text{NPO-WP}*}$) is constructed (see footnote 1; not shown). The advection of this first-order T_{850} signal by the climatological 850-hPa wind field (Fig. 5d) contributes significantly to the total NPO–WP temperature advection (the sum of Figs. 5b–d, shown in Fig. 5a). In fact, the temperature anomaly resulting from the total NPO–WP advection (with 3-day thermal damping) is somewhat larger than the T_{850} signal attributed to the NPO–WP (Fig. 1c). Clearly other terms

in the thermodynamic energy equation, such as the adiabatic and latent heating, are also important. The quasi-nonlinear advection term (Fig. 5c), however, is mostly unimportant relative to the other two advection terms.

4. Concluding remarks

A key element of the scientific method is seeking support for the proposed hypothesis by expanding the inquiry domain. After attributing the anomalously cold 2013/14 North American winter (and drought over the Pacific Northwest) to the heightened negative phase of the NPO–WP, we inquire if NPO–WP variability can be implicated in the generation of unusually warm North American winters as well. In March 2012, large swaths of central-eastern North America were warmer than normal by as much as 5°C and the Pacific Northwest was wetter by 25%–50% (see Fig. E6 in Climate Prediction Center 2012). Support for a prominent role of the NPO–WP (positive phase) in this warming episode follows from the large spatial anomaly correlation (-0.66) of this month’s T_{850} anomalies with the NPO–WP T_{850} regression pattern (Fig. 1c), footprint of the precipitation anomaly, and the striking similarity of the March 2012 300-hPa geopotential

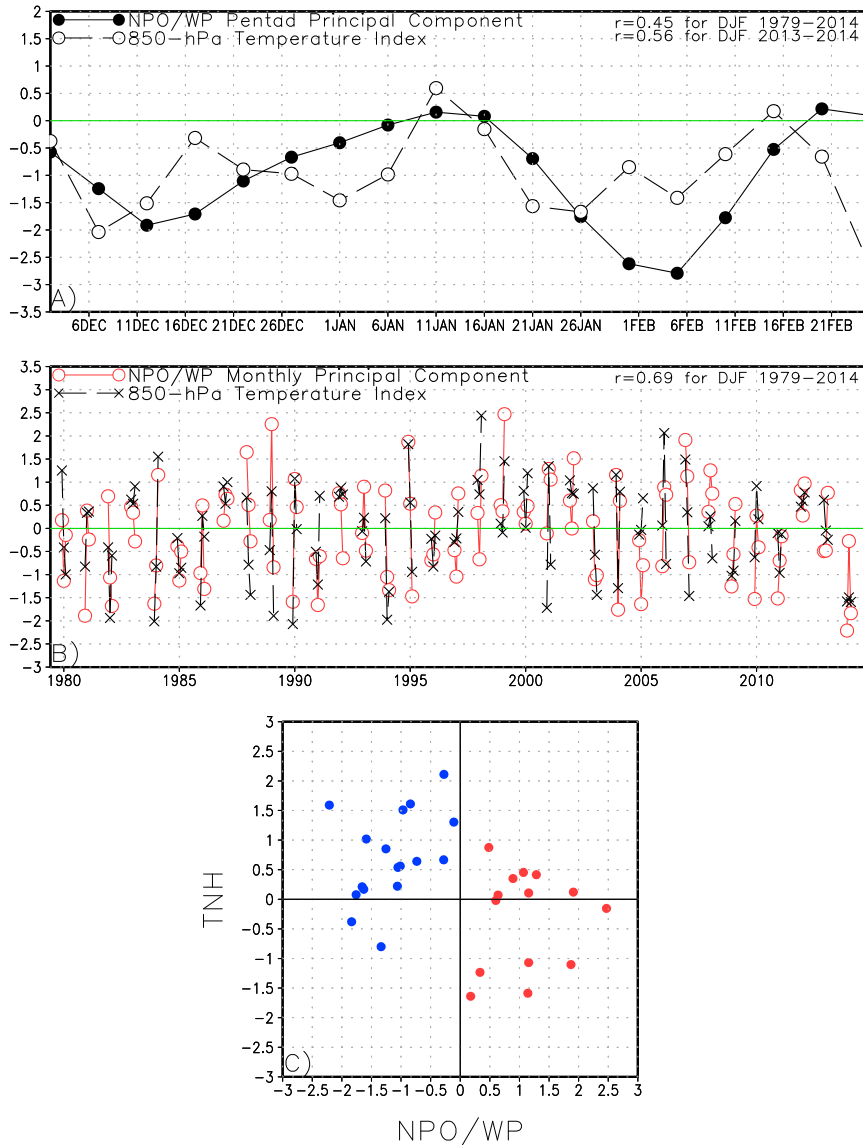


FIG. 4. (a) Pentad and (b) monthly distribution of the NPO–WP principal component and T_{850} over the northern Great Plains (marked box in Fig. 1); the top panel focuses on the recent winter (DJF 2013/14) while the middle panel covers the entire analysis period winters (1979–2014). The 200-hPa winter geopotential height (streamfunction) variability during 1979–2014 utilized for the seasonal (pentad) analysis, with correlation coefficients noted in the legend. (c) Scatterplot of the NPO–WP and TNH principal components from the 1979–2014 monthly analysis, when the T_{850} anomaly over the northern Great Plains exceeded plus or minus one standard deviation. Blue (red) dots denote cold (warm) winter months.

height (Z_{300}) anomalies (see Fig. S1 in Climate Prediction Center 2012) with the NPO–WP’s anomalies (Fig. 2c, but for the sign). The projection of the March 2012 Z_{200} anomalies onto the wintertime NPO–WP loading pattern was 1.24, a significantly positive value.

A pertinent question in context of this attribution is the longevity of the NPO–WP. A monthly analysis is likely to be too coarse for this estimation but a pentad-

resolution spatiotemporal analysis (e.g., Baxter and Nigam 2013) should suffice. This analysis yields 25 days as the duration time scale of a NPO–WP episode, based on the autocorrelation falloff to e^{-1} .

The origin of the NPO–WP remains enigmatic: concurrent links to the tropical SSTs are tenuous but linkage with extratropical SSTs (especially in the Gulf of Alaska) is strong in the monthly analysis (Nigam and Baxter 2015,

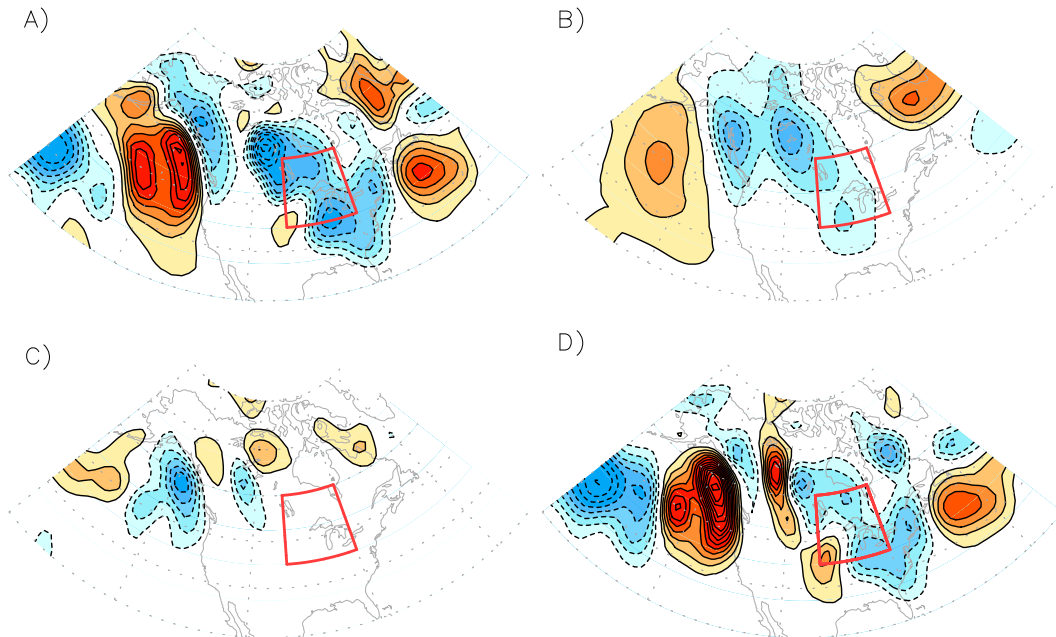


FIG. 5. Analysis of the NPO–WP related 850-hPa temperature advection: (a) total temperature advection from the sum of (b)–(d). (b) Advection of climatological temperature by NPO–WP related wind, that is, $\{-\mathbf{V}_a \cdot \nabla T_c\}_{850\text{hPa}}$, where \mathbf{V}_a is the NPO–WP wind anomaly and T_c is the climatological temperature. (c) Quasi-nonlinear term, $\{-\mathbf{V}_a \cdot \nabla T^{\text{NPO-WP*}}\}_{850\text{hPa}}$, where $T^{\text{NPO-WP*}}$ is derived from (b) using a 3-day thermal dissipation time scale (see footnote 1). (d) Advection of $T^{\text{NPO-WP*}}$ by the climatological wind, $\{-\mathbf{V}_c \cdot \nabla T^{\text{NPO-WP*}}\}_{850\text{hPa}}$. Note the contour interval and shading threshold is $3.86 \times 10^{-6} \text{ K s}^{-1}$ (zero contour omitted), a value that yields $\Delta T = 1.0 \text{ K}$ for a 3-day thermal dissipation time scale, facilitating comparison of (a) with Fig. 1c. A nine-point smoother is used to improve figure clarity in all panels.

their Fig. 9c); additional analysis, including SST-leading links, is warranted given the prominent role of NPO–WP in influencing North America’s winter hydroclimate. Interestingly, the Gulf of Alaska SSTs were notably positive in the 2013/14 winter (see Fig. T18 in Climate Prediction Center 2014; Izadi 2014), when the NPO–WP was strongly negative (cf. Fig. 4a) and Pacific storm tracks southward of their normal location (see Fig. E13 in Climate Prediction Center 2014).

Finally, this analysis cautions against succumbing to the post-1980–90s temptation of ascribing various extratropical anomalies in the Pacific–North American sector to ENSO—a favorite go-to mechanism because a causal inference can be drawn, unlike the extratropical rooted teleconnections whose origin and/or mechanisms remain to be elucidated. For example, a recent NOAA report on the causes and predictability of the California drought (Seager et al. 2014) utilizes climate modeling to suggest that the persistent, amplified circulation pattern over North America (the immediate synoptic-climate cause of the drought over California) may have been forced in part by the anomalously warm SSTs in the tropical western Pacific and related tropical convection. An influential role of these SSTs on North American winter climate is also highlighted in another recent study

(Hartmann 2015). Neither of these studies, however, provides process-level observational support (e.g., through OLR or diabatic heating analysis) for the posited causal link. The present study, with its emphasis on internal midlatitude variability, suggests that any tropical forcing is substantially weaker than the role of the NPO–WP, whose origin and evolution remain largely unknown, especially on seasonal time scales. This lack of mechanistic underpinning, however, does not make these teleconnections any less relevant in attribution analysis. Instead, a concerted research focus on their excitation, evolution, and longevity is warranted.

Acknowledgments. This analysis was undertaken during doctoral studies of the first author, who thanks NOAA’s Climate Prediction Center for supporting his doctoral pursuit. Sumant Nigam gratefully acknowledges support of NSF Grant AGS1439940.

REFERENCES

- Baxter, S., and S. Nigam, 2013: A subseasonal teleconnection analysis: PNA development and its relationship to the NAO. *J. Climate*, **26**, 6733–6741, doi:10.1175/JCLI-D-12-00426.1.
- Chen, M., P. Xie, J. E. Janowiak, and P. A. Arkin, 2002: Global land precipitation: A 50-yr monthly analysis based on gauge observations. *J. Hydrometeorol.*, **3**, 249–266, doi:10.1175/1525-7541(2002)003<0249:GLPAYM>2.0.CO;2.

- Climate Prediction Center, 2012: Climate Diagnostics Bulletin. March 2012, 90 pp. [Available online at http://www.cpc.ncep.noaa.gov/products/CDB/CDB_Archive_pdf/PDF/CDB.mar2012_color.pdf.]
- , 2014: Climate Diagnostics Bulletin. February 2014, 90 pp. [Available online at http://www.cpc.ncep.noaa.gov/products/CDB/CDB_Archive_pdf/PDF/CDB.feb2014_color.pdf.]
- Di Lorenzo, E., and Coauthors, 2013: Synthesis of Pacific Ocean climate and ecosystem dynamics. *Oceanography*, **26**, 68–81, doi:10.5670/oceanog.2013.76.
- Furtado, J. C., E. Di Lorenzo, B. T. Anderson, and N. Schneider, 2012: Linkages between the North Pacific Oscillation and central tropical Pacific SSTs at low frequencies. *Climate Dyn.*, **39**, 2833–2846, doi:10.1007/s00382-011-1245-4.
- Hartmann, D. L., 2015: Pacific sea surface temperature and the winter of 2014. *Geophys. Res. Lett.*, **42**, 1894–1902, doi:10.1002/2015GL063083.
- Izadi, E., 2014: The Gulf of Alaska is unusually warm, and weird fish are showing up. *Washington Post*, 15 September 2014. [Available online at <http://www.washingtonpost.com/news/speaking-of-science/wp/2014/09/15/the-gulf-of-alaska-is-unusually-warm-and-weird-fish-are-showing-up/>.]
- Lau, N.-C., 1979: The observed structure of tropospheric stationary waves and the local balances of vorticity and heat. *J. Atmos. Sci.*, **36**, 996–1016, doi:10.1175/1520-0469(1979)036<0996:TOSOTS>2.0.CO;2.
- Linkin, M. E., and S. Nigam, 2008: The North Pacific Oscillation–West Pacific teleconnection pattern: Mature-phase structure and winter impacts. *J. Climate*, **21**, 1979–1997, doi:10.1175/2007JCLI2048.1.
- Mo, K., and R. Livezey, 1986: Tropical-extratropical geopotential height teleconnections during the Northern Hemisphere winter. *Mon. Wea. Rev.*, **114**, 2488–2515, doi:10.1175/1520-0493(1986)114<2488:TEGHTD>2.0.CO;2.
- Nigam, S., 2003: Teleconnections. *Encyclopedia of Atmospheric Sciences*, J. R. Holton, J. A. Pyle, and J. A. Curry, Eds., Elsevier Science, 2243–2269.
- , and S. Baxter, 2015: Teleconnections. *Encyclopedia of Atmospheric Sciences*, 2nd ed. G. North, Ed., Elsevier Science, 90–109, doi:10.1016/B978-0-12-382225-3.00400-X.
- Palmer, T., 2014: Record-breaking winters and global climate change. *Science*, **344**, 803–804, doi:10.1126/science.1255147.
- Saha, S., and Coauthors, 2010: The NCEP Climate Forecast System Reanalysis. *Bull. Amer. Meteor. Soc.*, **91**, 1015–1057, doi:10.1175/2010BAMS3001.1.
- Seager, R., M. Hoerling, S. Schubert, H. Wang, B. Lyon, A. Kumar, J. Nakamura, and N. Henderson, 2014: Causes and predictability of the 2011–14 California drought, Assessment Rep., NOAA, 40 pp. [Available online at http://cpo.noaa.gov/sites/cpo/MAPP/Task%20Forces/DTF/californiadrought/california_drought_report.pdf.]
- Walker, G. T., 1924: Correlation in seasonal variations in weather IX: A further study of world weather. *Mem. Indian Meteor. Dept.*, **24**, 275–332.
- Wallace, J. M., and D. S. Gutzler, 1981: Teleconnections in the geopotential height field during the Northern Hemisphere winter. *Mon. Wea. Rev.*, **109**, 784–812, doi:10.1175/1520-0493(1981)109<0784:TITGHF>2.0.CO;2.